Meteorology and Atmospheric Physics (2022) 134:19
https://doi.org/10.1007/s00703-021-00855-5

ORIGINAL PAPER

Spatio-temporal variations of tropospheric nitrogen dioxide in South Mato Grosso based on remote sensing by satellite

Amaury de Souza[1] · Flavio Aristone[1] · Marcel Carvalho Abreu[1] · José Francisco de Oliveira-Júnior[1] · Widinei Alves Fernandes[1] · Ivana Pobocikova[1]

Received: 16 July 2021 / Accepted: 13 December 2021 / Published online: 20 January 2022

Abstract

The study evaluates the characteristics of tropospheric nitrogen dioxide (NO_2) concentrations from 2005 to 2020 in eight cities in the State of Mato Grosso do Sul (MS), Midwestern Brazil, using data available from the Ozone Monitoring Instrument (OMI). The average concentration varies from 2981×10^{15} molecules/cm^2 in Campo Grande, where commercial, industrial and vehicular activities take place, to 2906×10^{15} molecules/cm^2 in Corumbá and 3035×10^{15} molecules/cm^2 in Porto Murtinho, regions of livestock and biomass burning. The results, based on the Mann–Kendall (MK) test, show a significant increase ($p < 0.05$) in the NO_2 column levels in the region. For each of the eight cities studied, a significant seasonal cycle of NO_2 columns was determined. The maximum value of NO_2 concentration was observed in the dry period, from July to September, while the minimum value was registered in the rainy period, from October to March.

1 Introduction

Nitrogen dioxide (NO_2) is a reactive and short-lived gas, with natural and anthropogenic sources, are harmful contaminants, as they are associated with adverse effects on human health, especially with regard to respiratory diseases, and the environment (Souza et al. 2018a, b). The main sources of NO_2 are fossil fuel combustion, biomass burning, soil emissions and lightning (Hagenbjörket et al. 2017). NO_2 is a toxic air pollutant in the high-concentration condition and plays an important role in tropospheric chemistry as a precursor of tropospheric ozone and secondary aerosols (Jiang et al. 2021; Fan et al. 2021; Castellanos and Boersma 2012; Grajales and Baquedo-Bernal 2014; Fantozzi et al. 2015; Griffin et al. 2018; Xue et al. 2020; Nakada and Urban 2020). Observations of the space–time variations of NO_2 form the basis for understanding the spatial distributions and temporal trends of NO_2. Nonetheless, the limitation on insufficient spatial and temporal coverage of ground-level monitoring networks is the main challenge to understand the NO_2 dynamics in the atmosphere.

Many techniques and methods have been used successfully in monitoring atmospheric NO_2 based on in situ surface measurements, remote sensing from satellite sensors and ground-based instruments (Xiao et al. 2018; Drosoglou et al. 2018). Although in situ measurements and remote sensing of ground-based instruments show high accuracy and precision, their usefulness in determining the spatiotemporal distributions of trace gases is limited due to their sparse spatial and temporal coverage. Space-based measurements provide information on large-scale NO_2 distributions and in areas where in situ and ground-based systems cannot be easily deployed (Lamsal et al. 2010). Measurement of atmospheric NO_2 is ordinarily obtained from in situ data of air quality stations (AQS) (Fan et al. 2020). However, AQS lack space–time coverage, particularly in countries like Brazil, where measurements are restricted to metropolitan regions (MR)—(Zeri et al. 2011, 2016). On the other hand, the data obtained via Remote Sensing provide data with larger spatiotemporal coverage in relation to AQS and without failures or discontinuities in their time series. Satellite observations provide NO_2 data from the total tropospheric column over an area, while AQS measures locally (Richter et al. 2005).

The first NO_2 monitoring in the troposphere started in 1995 using the Global Ozone Monitoring Experiment (GOME) on the European Remote Sensing Satellite-2

Responsible Editor: Sang-Woo Kim.

Amaury de Souza
amaury.de@uol.com.br

[1] Universidade Federal de Mato Grosso do Sul, Campo Grande, MS, Brazil

(ERS-2). Ozone Monitoring Instrument (OMI) started aboard the Aura satellite in 2002, and in 2004 the new GOME-2 began to collect data. The Tropospheric Monitoring Instrument (TROPOMI) aboard the Precursor Copernicus Sentinel-5 satellite started in 2017. The OMI measures atmospheric NO_2 daily since late 2004 with spatial resolution of 13 × 24 km in the nadir visualization, increasing the size to 24 × 135 km for widest viewing angles. Several studies have been performed using satellite observation data of tropospheric NO_2 columns (Richter et al. 2005; Castellanos and Boersma 2012; Schneider and Van Der 2012; Lelieveld et al. 2015; Khokhar et al. 2015; Irie et al. 2016; Cai et al. 2018; Yanfang et al. 2019; Yavaşlı 2020; Zheng et al. 2018), and they show that its concentrations are dependent on economic, industrial, and other human-controlled activities but not correlated to emission policies to improve air quality. Several inventories on both global and regional scales of NO_2 concentrations normally use regression models for trending analysis. Nevertheless, verification of tropospheric NO_2 trends has not yet been carried out for the State of MS, Brazil. In this paper, the tropospheric concentration of NO_2 is analyzed for the period 2005–2020 throughout the available OMI data. It has been highlighted of the characteristics of the spatial distribution of NO_2 using the Kendall seasonal test for each pixel.

2 Materials and methods

2.1 Area of study and meteorological data

The State of MS is located in the Midwest Region of Brazil and encompasses approximately 358,159 km^2, see Fig. 1a. It is known for its agricultural activities, the main economic products of MS being soybean and beef cattle production. The State topography is represented in Fig. 1b and shows elevation ranging from 24 to 1100 m (Teodoro et al. 2016).

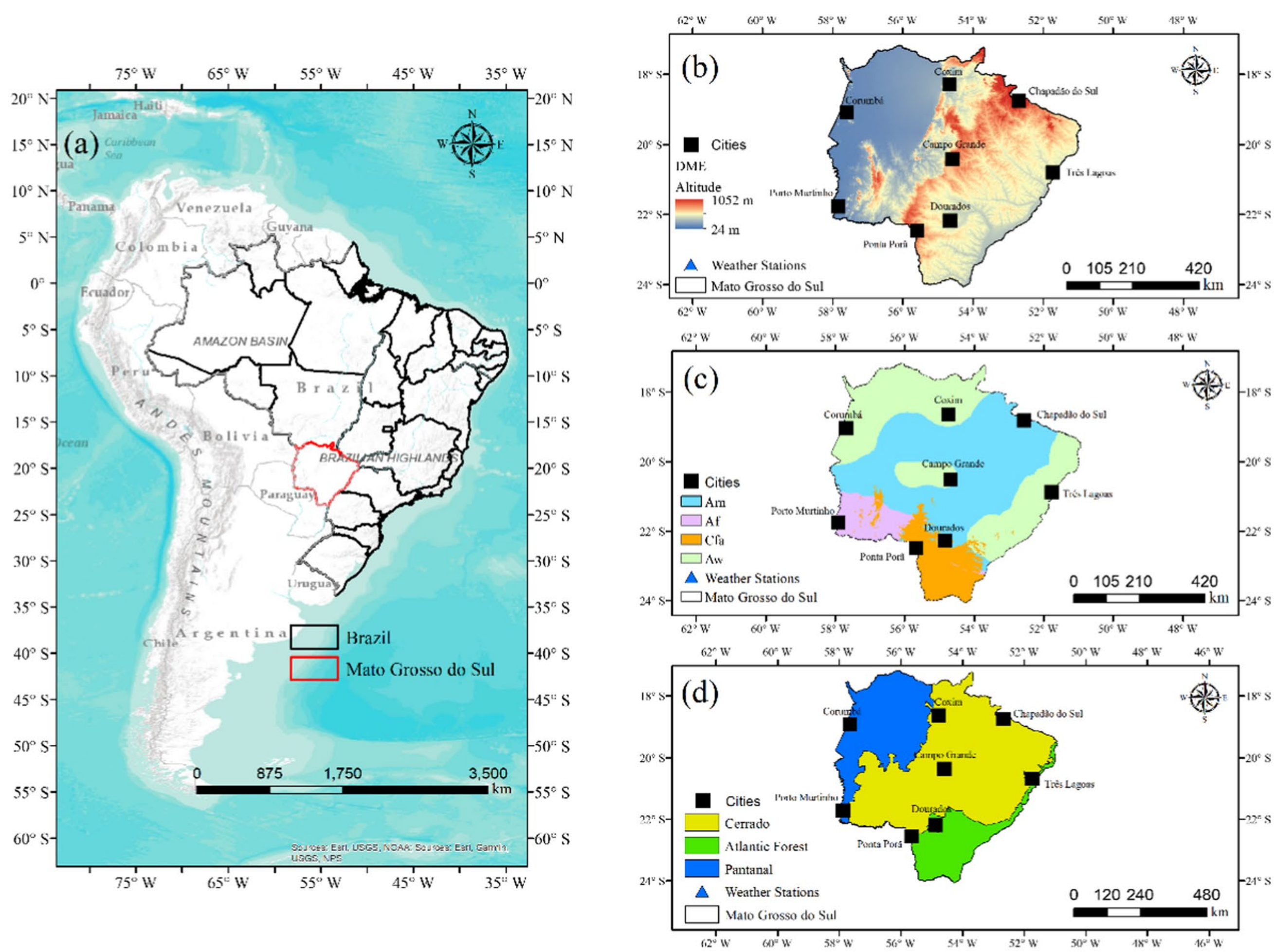

Fig. 1 South Mato Grosso State in Brazil. **a** Model of Digital Elevation (MDE); **b** climate classification by Köppen; **c** biomes; **d** localization of studied cities

The average annual temperature varies from 20 to 26 °C, and the mean annual rainfall ranges from 1000 to 1900 mm. The climate presents well-defined dry seasons from April to September, when the higher rainfall records are observed in the southern portion of the state. The rainy season goes from October to March, the northern region of the State receives higher rainfall records compared to the southern region. The Köppen's classification divides the climate diversity of MS into several regions: (1) "Aw" in the Southeast and Northern parts of the state; (2) "Am" for the central region; (3) "Af" in the Southwest; and (4) "Cfa" in the Southern, see Fig. 1c. In the Southwest portion of MS, south of the Pantanal region, which lies between − 21° and − 22° latitude, the climate is characterized as tropical forest ("Af"), with rainfalls distributed throughout the year. The central portion of the State is predominantly characterized by tropical monsoon climate ("Am"), with a small dry season during winter. In the northern part, in a small portion of the central region, and the Southeastern region of the state, the climate is characterized as savannah ("Aw"), which tends to present dry winters and rainy summers. Only in the Southern of the state, the climate is humid during all seasons ("Cfa"), with hot summers and average temperatures above 22 °C (Souza et al. 2012; Alvares et al. 2013).

The biome diversity of MS is represented in Fig. 1d. It includes areas of the Atlantic Forest, the Cerrado, and the Pantanal with 14%, 61%, and 25% of the state-encompassed area. The Atlantic Forest is particularly an important biome due to its abundant biological diversity. It has gained substantial interest as a conservation area since this biome has been considerably reduced in the past. The Brazilian Cerrado is a vast tropical savanna ecoregion widely known for its native habitats and rich biodiversity. It represents the second largest biome in South America, after the Amazon. The Cerrado of South Mato Grosso is located in two hydrographic regions of Brazil, represented by the rivers Parana and Paraguay. The Pantanal is the world's largest inland flooded grasslands and savannas wetland region. It is home to rich wildlife and worldwide known for its unique biome. The region is considered delicate regarding biodiversity due to environmental degradation and damage (Teodoro et al. 2016).

Eight cities of South Mato Grosso have been studied in this paper. These cities are, the State capital Campo Grande, Chapadão do Sul, Corumbá, Coxim, Dourados, Ponta Porã, Porto Murtinho, and Três Lagoas, all represented in Fig. 1. They have been chosen accordingly the availability of meteorological and NO_2 concentration data, expressed in 10^{15} molecules/cm^2, for the period from 2005 to 2020. The meteorological data series have been collected from the Brazilian National Water Agency (ANA) database, from Hidroweb (www.snirh.gov.br/hidroweb/publico/medicoes_historicas_abas.jsf), and from the Brazilian National Institute of Meteorology (INMET) (www.inmet.gov.br), all accessed in in January 2021. The data include time series of maximum and minimum air temperature, i.e., T_{max} and T_{min}, respectively, relative humidity (RH) in %, and precipitation (Prec) in mm. A summary of the meteorological conditions for the studied period is presented in Table 1.

The eight cities have different characteristics related to geographic position, population and main economic activities, as follows: (1) Coxim, located in the Cerrado region of influence, with small patches of open fields. It presents itself in its different physiognomies and in enclaves with the Seasonal Forest. The planted pasture is expressive in the central portion of the municipality. Its economy is strongly linked to fishing, culture, livestock and agriculture tourism; (2) Três Lagoas, the predominant vegetation is the Cerrado with strips of Atlantic Forest. Its economy is strongly linked to fishing, livestock and pulp tourism. It is the third most populous city in MS State, with a population of around 123,000 inhabitants; (3) Campo Grande, the State capital, is located on the watershed of the Paraná and Paraguay River basins. The Guarani Aquifer passes under the city, being the capital of the State holding the largest percentage of the Aquifer within the Brazilian territory, the predominant vegetation being the Cerrado. Its economy is strongly linked to tourism and agriculture. It is the third largest and most developed urban center in the Midwest Region of Brazil, and the most populous city in MS and the 19th most populous in Brazil; (4) Chapadão do Sul, located in the Cerrado region

Table 1 Weather stations in South Mato Grosso: cities, latitude (°), longitude (°), altitude (m), minimum and maximum temperatures (°C), average and standard deviation of precipitation (mm), and number of inhabitants

City	Lat (°S)	Lon (°W)	Alt (m)	T_{min} (°C)	T_{max} (°C)	Prec (mm)	Inhab
Coxim	− 18.51	− 54.76	238	22.4 ± 2.33	30.29 ± 9.08	1350.6 ± 60.18	33,459
Três Lagoas	− 20.75	− 51.68	319	20.71 ± 2.66	30.77 ± 2.67	1229.8 ± 83.00	123,281
Campo Grande	− 20.44	− 54.65	712	19.89 ± 2.34	27.49 ± 8.21	1422.3 ± 191.73	792,252
Chapadão do Sul	− 18.79	− 52.62	786	19.48 ± 2.35	27.3 ± 8.16	1684.8 ± 212.32	25,865
Ponta Porã	− 22.54	− 55.73	755	18.48 ± 2.76	25.91 ± 7.76	1530.9 ± 203.98	93,937
Corumbá	− 19.01	− 57.65	118	22.34 ± 2.91	30.88 ± 9.19	1519.1 ± 27.8	12,058
Porto Murtinho	− 21.70	− 57.88	90	22.77 ± 2.23	30.64 ± 9.19	1306.2 ± 20.65	17,298
Dourados	− 22.22	− 54.81	430	19.26 ± 2.99	27.55 ± 8.22	1455.8 ± 113.7	225,495

of influence, in the northeast of the State of MS. It is one of the cities of MS State with the highest altitude (around 900 m) and population around 25 thousand inhabitants. (5) Ponta Porã, on the border with Paraguay, with predominance of clean fields, formed by large areas of low grass, constituting the famous natural pastures. Its economic activities are cattle raising, agriculture, wood extraction. Ponta Porã is in the Cerrado area, but in transition with the Mata Atlantica biome. The population is approximately 95,000 inhabitants; (6) Corumbá, on the border with Paraguay and Bolivia, in a Pantanal biome region with a rich and varied vegetation, which includes the typical fauna of other Brazilian biomes, such as the Cerrado, the Caatinga and the Amazon region. The nutritious sludge layer that remains in the soil after flooding allows for the development of a rich flora. In areas where floods dominate, but which are dry during the winter, vegetations, such as carandá and paratudal palms, occur. Its economy is quite diversified, highlighting the activities of mining, fishing and tourism, and agriculture. The highest rates of fires in MS occur in the region of Corumbá. The population of Corumbá is 112,000 inhabitants. (7) Porto Murtinho, in the Pantanal biome, in a transition area with the Cerrado, distributed almost equitably, the coverage is typical of the Pantanal (Cerrado Estépico). There is also cultivated pasture and some crops, the most representative activity is agriculture and was a great producer of mate. The population of Porto Murtinho is around 15,000 inhabitants. (8) Dourados, its natural vegetation is clear fields, also having large parts of Cerrados and large patches of tropical forests, since it is located in area Atlantic Forest area but in a transition area Atlantic Forest–Cerrado. Its economy is mainly based in agriculture and planted pasture. It is the most populous city in the interior of MS State, with a population of approximately 228,000 inhabitants.

2.1.1 OMI sensor data

For the analysis, data were collected in grid format with spatial resolution of $1^\circ \times 1^\circ$ and daily temporal resolution referring to areas in the regions of Mato Grosso do Sul aboard the Aura satellite in 2004. The main objective of the OMI is to obtain global measurements at high spatial and spectral resolution of a series of trace gases in the troposphere and stratosphere (Levelt et al. 2006). It can distinguish between types of aerosols, such as smoke, dust and sulfates (Duncan et al. 2013). According to Torres et al. (2013), this is done through the OMAERUV algorithm that uses pre-computed reflectance from the upper atmosphere for a set of 21 aerosol models composed of three types of aerosols (dust, carbonaceous aerosols, sulfate-based aerosols).

As described on the project's own page, the OMI is a nadir imaging spectrograph that measures solar radiation backscattered by the Earth's atmosphere and surface over the entire wavelength range from 270 to 500 nm with a spectral resolution of about 0.5 nm. The ratio of the calibrated radiance and irradiance is equal to the Earth's atmospheric bidirectional scattering distribution function (BSDF). Light entering the telescope is depolarized using a scrambler and then split into two channels: the UV channel with a wavelength range 270–380 nm and the VIS channel with a wavelength range 350–500 nm (Levelt et al. 2006). These factors are important to obtain the concentration of trace gases and to allow the IMO to monitor tropospheric pollution phenomena, such as biomass burning and industrial pollution, as the tropospheric pollution record is essential to study the human impact on the Earth's atmosphere and climate (Dobber 2006).

2.2 Preliminary analysis

The preliminary analyses consist of establishing position and dispersion statistics of notched box-plot for the NO_2 concentration. The medians obtained for the listed cities in MS on a monthly scale are then compared.

2.3 Trend analysis of NO_2 concentration

The trend analysis has been applied to the monthly data. The Mann–Kendall (MK) non-parametric test (Mann 1945; Kendall 1975) has been applied to define the trend. The linear regression analysis to verify the proportion of increase or decrease of the response variable is based on the slope of the characteristic function. The Pettitt test (1979) has been applied to verify the point of interruption of the line (beginning of the trend). The estimated slope of the trend is calculated using a generalized version of Sen's slope estimator (Sen 1968).

The MK is the trend verification test recommended by the World Meteorological Organization (WMO), widely used in hydrological studies (Burn et al. 2011; Sa'adi et al. 2019). It tests whether the series presents a downward or upward trend. The null hypothesis means that there is no trend. For a time series, the Mann–Kendal (S) statistic is defined by:

$$S = \sum_{k=1}^{n-1} \sum_{i=k+1}^{n} \operatorname{sgn}\left(x_i - x_k\right) \tag{1}$$

where x_i is the i-th observation and x_k is the k-th observation immediately after the i-th observation, n is the number of elements in the time series. The variance is determined by the following relationship:

$$\operatorname{Var}(S) = \frac{n \cdot (n-1) \cdot (2n+5) - \sum_{i=1}^{m} t_i(t_i - 1) \cdot (2 \cdot t_{i+5})}{18} \tag{2}$$

where m is the number of tied groups, t_i is the number of loop lengths equal to i.

The MK test requires that the sample data are serially independent, i.e., absence of autocorrelation. Correlated sample data in series affect the test ability to correctly assess the significance of the trend. To eliminate any effect of serial correlations in the MK test, autocorrelation analysis has been performed. A correlogram gives a summary of correlations at different periods of time. It consists of the graphic analysis of the autocorrelation function for sequential values of delay $k = 0, 1, 2, \ldots, n$. In the occurrence of verified autocorrelation, the MK test was applied with the modification proposed by Yue and Yang (2004). This modification involves a variance correction to address the issue of serial correlation in the trend analysis, maintaining the significance of the test (Sa'adi et al. 2019).

Regression analysis provides the trend rate using the slope of the resulting function. The slope value indicates the magnitude of the trend while the sign (±) indicates an increase or decrease behavior of the tested variable. However, the slope must be confirmed by the Student's t test for statistical significance, i.e., whether it differs from zero or not.

The Pettitt test (1979) uses the Mann–Whitney $U_{(t,\,M)}$ statistic to verify whether two samples belong to the same population. Thus, the test places the data series in two samples: $x_1, x_2, \ldots, x_t$ and $x_{t+1}, x_{t+2}, \ldots, x_n$, to calculate $U_{(t,\,M)}$ as follows (Kengni et al. 2019):

$$U_{(t,n)} = U_{(t-1,n)} + \sum_{j=1}^{n} \operatorname{sgn}\left(x_t - x_j\right) \quad (3)$$

with:

$$\operatorname{sgn} = (x)\begin{cases} 1, & \text{when } x > 0 \\ 0, & \text{when } x = 0 \\ -1, & \text{when } x < 0 \end{cases} \quad (4)$$

Pettitt statistics account for the number of exceedances in which the value of the first sample exceeds that of the following sample. The null hypothesis of the test is that there is no breaking point in the data series. The level of significance is adopted 5%, as assumed by other authors (Uliana et al. 2015).

2.4 Principal components of NO_2 concentration

Principal component analysis (PCA) was performed to explain the variance structure of the data through linear combinations of the original variables. The variables used were: NO_2 concentration (10^{15} molecules/cm^2), maximum (T_{max}) and minimum (T_{min}) temperature of the air (°C), (RH) relative humidity (%), and (Prec) precipitation (mm) for the MS cities. PCA allows the use of variables correlated with each other, to form components capable of explaining the variance of the data. The main components were extracted using the correlation matrix between the variables (Shi and Harrison 1997).

PCA was used after calculating the Kaiser–Meyer–Olkin (KMO) index. Bartlett's sphericity tests were first performed to confirm the adequacy of PCA to the NO_2 concentration and meteorological data. The KMO test verifies the correlation measure of the independent variables. The value of the test varies from 0 to 1, whereas values below 0.5 indicate that the application of PCA is inappropriate. The Bartlett's test of sphericity evaluates whether the correlation matrix is an identity matrix, which would indicate that there is no data correlation, indicating that the factorial model is inappropriate.

3 Results and discussion

3.1 Preliminary analysis—descriptive statistics

The position and statistic dispersion of the NO_2 tropospheric concentration data are presented in Table 2. The box-plot displaying the monthly distribution of the tropospheric NO_2 concentration in the MS studied cities between 2005 and 2020 is exhibited in Fig. 2. The city of Campo Grande present as average of NO_2 concentration 2.98×10^{15} molecules/cm^2, and the median 2.87×10^{15} molecules/cm^2. Ponta Porã, which is in the south of the State and borders Paraguay, registered higher values: 3.038×10^{15} and 2.935×10^{15} molecules/cm^2 as average and median, respectively. Porto Murtinho, located in the west of the State of MS and on the border with Bolivia, registered the second-highest mean 3.035×10^{15} molecules/cm^2 and median 2.814×10^{15} molecules/cm^2. The distribution of data points over the 15 years shows that, in addition to each city being uniquely identifiable, Ponta Porã and Porto Murtinho exhibit some heavy tail properties. The resulting parameters of asymmetry and kurtosis (Skew, kurtosis) for these cities are the largest in comparison to the other studied cities.

NO_2 concentrations in the State of MS indicated less seasonal amplitude among the annual averages of 0.20×10^{15} molecules/cm^2, with higher values in July, August and September, and constant values between January and June (Fig. 2). From October to December, there is a decrease in NO_2 concentration, probably due to the excessive use of power plants and domestic heating, which increase the NO_2 levels during the winter. Another point is the burning of fields in the region to clean the pastures (Caúla et al. 2015; Oliveira Júnior et al. 2020).

The notch box-plot shows differences between some of the cities in their medians, since the notches do not overlap.

Table 2 Descriptive analysis of the historical NO_2 series concerning the studied cities of State MS (Campo Grande, Dourados, Três Lagoas, Corumbá, Coxim, Porto Murtinho, Ponta Porã and Chapadão do Sul) for the period from 2005 to 2020

Cities	Mean	SD	CV (%)	Minimum	Q1	Median	Q3	Maximum	Skewness	Kurtosis
Campo Grande	2.98	0.40	13.33	2.30	2.69	2.87	3.21	4.27	0.90	0.39
Dourados	2.99	0.40	13.47	2.18	2.69	2.90	3.24	4.26	0.73	0.16
Três Lagoas	2.94	0.40	13.45	2.11	2.65	2.87	3.17	4.41	0.69	0.23
Corumbá	2.91	0.70	24.09	1.96	2.46	2.64	3.22	5.56	1.66	2.56
Coxim	2.95	0.49	16.50	2.26	2.59	2.85	3.26	5.02	1.20	1.72
Porto Murtinho	3.04	0.67	22.19	1.99	2.56	2.82	3.36	6.08	1.46	2.66
Ponta Porã	3.04	0.51	16.83	2.10	2.66	2.94	3.35	5.61	1.33	3.08
Cachoeira do Sul	2.95	0.42	14.32	1.94	2.63	2.90	3.18	4.32	0.67	0.34

SD standard deviation, *CV* coefficient of variation, *Q1* quartile 25%, *Q3* quartile 75%.

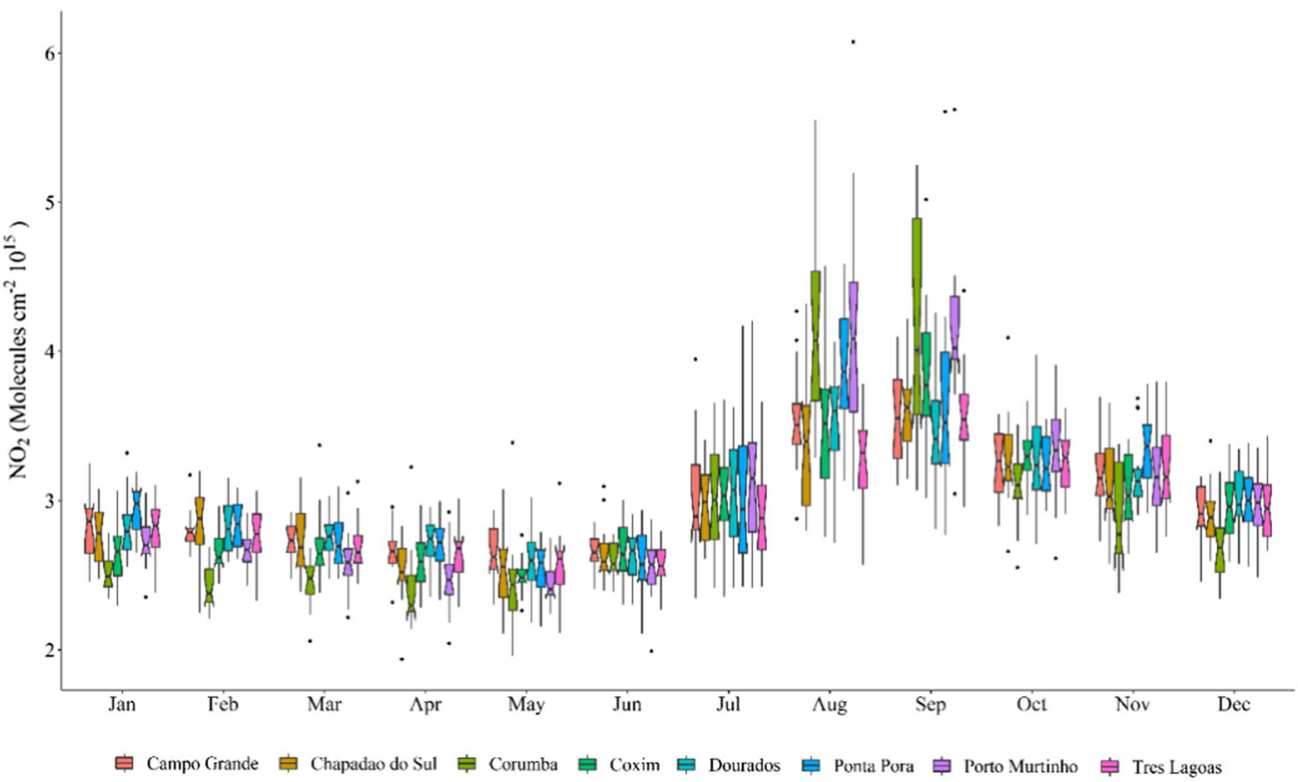

Fig. 2 Notch box-plot for monthly tropospheric NO_2 concentration in cities of South Mato Grosso State, Brazil

Ponta Porã presents higher median, especially from January to August, while Dourados shows increase of the median from September to December. Both cities are located in the south portion of the MS, at the boundary between the Cerrado and the Atlantic Forest biomes, where the crops and pasture are expressive economic activities (Tomei et al. 2020). All the cities displayed a delay of one or two months in relation to the highest concentrations of NO_2, from July and October relative to the driest months, from June to September (Teodoro et al. 2016; Abreu et al. 2020). Cities in the north–northwestern portions of the State of MS present lower medians. It is the case of Coxim, located in the transition between the Pantanal and the Cerrado, and Chapadão do Sul, in the Cerrado. These cities have lower crop density and lower fire foci (Oliveira-Júnior et al. 2020), which may contribute for lower concentrations of NO_2. The fires are associated with the cleaning of areas for agriculture and contribute to increase the concentrations of NO_2.

In contrast, the monthly behavior demonstrates similarity between the concentration of NO_2 in the cities throughout the year, with a higher NO_2 concentration between July and November, reaching the maximum values in August and

September. NO_2 concentrations in October begin to decrease until reaching their minimum values during April and May. This behavior is in agreement with the distribution of precipitation distribution in South Mato Grosso (Teodoro et al. 2016; Abreu et al. 2020). From December through March, the northern portion where the cities of Corumbá, Coxim, Três Lagoas, and Chapadão do Sul are located (Fig. 1) presents higher precipitated totals. From May through September, southern region where the cities of Dourados, Ponta Porã, and Porto Murtinho are located presents higher precipitated totals. From April through October, i.e., during the transition months, the influence of the orography on the larger precipitations is marked along the longitudinal direction south/northeast. This pattern indicates that NO_2 concentrations are higher during dry periods in cities. The NO_2 variability is linked to the meteorological conditions (Ul-Haq et al. 2018). Nevertheless, this pattern is not the only influence affecting the observed values of concentrations. In fact, the raining deposited by precipitation can significantly reduce the amount of pollutants in the atmosphere (Feng et al. 2001; Garrett et al. 2010; Zhao et al. 2020).

The anthropic action of using fire to clean areas for planting agricultural commodities in the rainy season (Silva Junior et al. 2020) occurs during the dry period, mainly in the months of August and September. This period precedes the rainy season, which begins in October (Teodoro et al. 2016; Abreu et al. 2020). The burning of biomass has been reported as one of the responsible factors to increase the NO_2 concentrations in some periods of the year (Ossohou et al. 2019). The effect of seasonality is therefore related to anthropogenic human activities, not exclusively natural events.

3.2 Analysis of trends in NO_2 concentrations

The analysis of the NO_2 levels data series showed autocorrelation and trends for the studied period, as detected by the modified MK test. The cities of Dourados and Porto Murtinho showed decrease in NO_2 concentrations, Coxim presented increase instead, considering all the monthly data exhibited in Table 3. Calculation of Sen's inclinations of significant trends indicate changes up to $\pm 0.001 \times 10^{15}$ molecules/cm^2. These trends changed approximately 1% on average. In terms of magnitude, the cities of Dourados and Porto Murtinho decreased by 0.084×10^{15} and 0.064×10^{15} molecules/cm^2 respectively, while in Coxim, there was an increase of 0.095×10^{15} molecules/cm^2. These results are expressed in Fig. 3.

Additional relevant aspects about the concentrations of NO_2 in the studied period are the peaks and valleys in several areas in the MS. In general, the effects of the 2008 global economic crisis can be observed during the period 2009–2011 in most of the assessed cities. Therefore, variations in the measurements during this period are associated with depletion in industrial production. The blocking measures due to COVID-19 in 2020 affected industries, transports, and other human activities in Brazil and many other countries. Therefore, emissions of air pollutants during the pandemic have been drastically reduced in several countries (Zhang et al. 2021; Wang et al. 2021). In Brazil, the impact of COVID-19 containment actions in terms of air pollutants is still being evaluated. In this study, reductions of the averaged NO_2 concentrations have been observed during 2020 compared to the period from 2005 to 2019 in only two cities, Dourados and Três Lagoas, in the order of 0.02×10^{15} and 0.03×10^{15} molecules/cm^2. In the other studied cities, higher concentrations of NO_2 have been observed during 2020, with an average of 0.01×10^{15} to 0.22×10^{15} molecules/cm^2, see Table 4. Therefore, although for some months of 2020, the concentration of NO_2 was lower, in general it was higher compared to the period from 2005 to 2019. These results suggest the general non-commitment of the containment values during the pandemic in Brazil, which may have contributed to the excessive number of deaths, since the relationship between COVID-19 and its mortality with the concentration of NO_2 in the atmosphere has been evidenced. The concentration of NO_2 as a precursor to the formation of secondary particulate material may favor COVID-19 and make the respiratory system more susceptible to this infection (Mele et al. 2021).

Figure 4 shows the monthly dispersion of NO_2 concentration as a function of time in years, and the regression curves where most of the cases can be observed. The MK test for the monthly data series shows some trends for specific months. In addition, during the dry period in MS, which is from April to October, some relevant trends have been detected. Increase trends are observed for Corumbá in July and for Coxim in July, August, and December. These cities are located in the driest area of South Mato Grosso

Table 3 Result of the Mann–Kendall test for detecting trends in daily NO_2 series in eight cities in South Mato Grosso

City	*Z*	*p* value	Tau	Sen's slope	Break point
Campo Grande	0.522	0.601	0.011	1.27E − 04	–
Dourados	− 2.449	0.014*	− 0.034	− 3.05E − 04	Nov/2017
Três Lagoas	− 1.075	0.282	− 0.018	− 1.77E − 04	–
Corumbá	− 0.225	0.822	− 0.004	− 4.72E − 05	–
Coxim	4.679	0.000*	0.078	8.84E − 04	May/2013
Porto Murtinho	− 2.286	0.022*	− 0.035	− 4.56E − 04	Dec/2010
Ponta Porã	− 1.75	0.08	− 0.027	− 3.00E − 04	–
Chapadão do Sul	0.063	0.949	0.001	6.86E − 06	–

*Within 5% level of significance

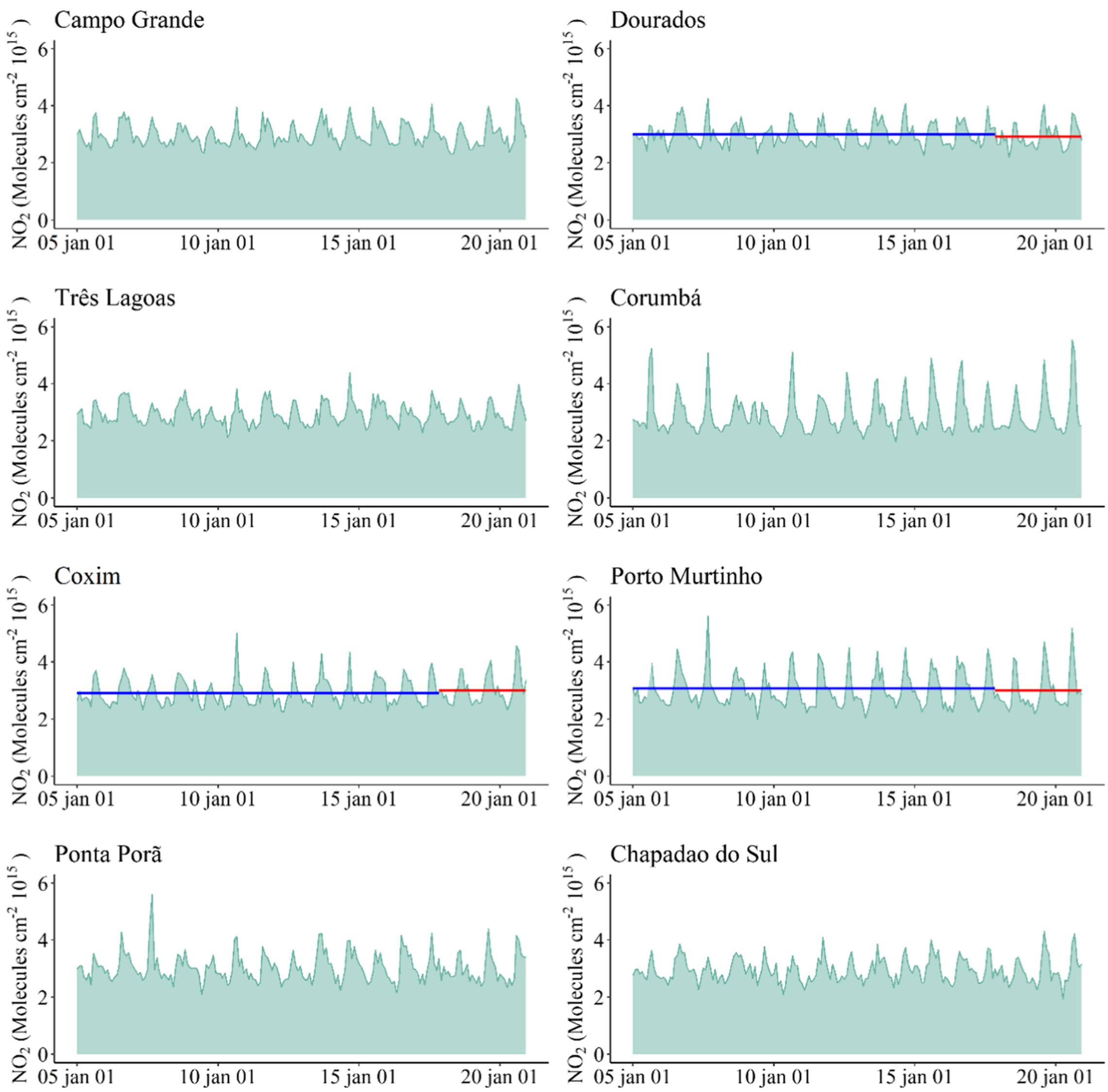

Fig. 3 Time series of NO_2 concentration in the eight cities of South Mato Grosso. The blue line represents the mean before and the red line the mean after the break point of the series

(Abreu et al. 2020) and in the Pantanal biome. The exception is Chapadão do Sul that is located in the Cerrado biome. Oliveira-Junior et al. (2020) detected higher occurrence of fire foci in relation to the Cerrado and the Atlantic Forest areas. Decrease trends have been observed for Corumbá in January, for Dourados in May, and for Porto Murtinho in April and May.

With the exception of Chapadão do Sul, the decreasing trends in the NO_2 concentrations during April and May may be associated with the characteristics of precipitation in the southern region of the state, in which there are higher total precipitates (Abreu et al. 2020). There is a noticeable relationship connecting the environmental impact of agricultural expansion and fires to the NO_2 concentrations. Although few trends have been detected, they occurred in months of area cleaning activities with the use of fires that result in large emissions of gasses, include NO_x, which contribute to increase the greenhouse gas emissions and global warming (Oliveira-Junior et al. 2020).

Table 5 shows the MK test results, Tau, Sen's slope, and the break point, i.e., the year of change by the Pettitt test validating a significant trend in MK test. The changes indicated an increase of NO_2 concentration between 0.03×10^{15} and 0.070×10^{15} molecules/cm^2, especially in drier months for cities in the south of the State of MS. The decrease of values varied between 0.02×10^{15} and 0.04×10^{15} molecules/cm^2. The break points in the monthly series occurred from 2010 to 2014, i.e., from the first to the third quartile of the data series.

Table 4 Monthly and annual average of concentration of NO_2 in the refereed cities of South Mato Grosso, Brazil from 2005 to 2019 and 2020

Period	Month	Campo Grande	Dourados	Três Lagoas	Corumbá	Coxim	Porto Murtinho	Ponta Porã	Chapadão do Sul
2005–2019	Jan	**2.80**	**2.79**	2.82	2.52	**2.64**	2.75	2.95	**2.75**
	Feb	**2.79**	**2.83**	2.74	2.42	**2.65**	2.68	2.85	**2.85**
	Mar	2.73	**2.75**	2.72	2.46	2.69	2.59	2.73	2.74
	Apr	**2.65**	2.73	2.65	2.41	2.60	**2.47**	2.71	2.58
	May	2.65	2.62	2.59	2.45	**2.49**	**2.44**	**2.52**	**2.55**
	Jun	2.67	2.65	2.58	**2.59**	**2.65**	2.56	2.60	2.64
	Jul	3.05	3.05	**2.91**	**3.00**	**3.00**	**3.14**	3.05	2.98
	Aug	**3.50**	**3.55**	**3.25**	**4.06**	**3.43**	4.08	**3.86**	**3.36**
	Sep	**3.51**	**3.43**	**3.53**	**4.09**	**3.83**	4.15	**3.65**	**3.56**
	Oct	**3.21**	**3.25**	**3.24**	3.11	3.28	3.38	**3.22**	3.29
	Nov	**3.17**	3.19	3.25	2.91	3.06	3.15	**3.35**	3.11
	Dec	2.93	3.02	2.98	2.71	2.94	2.98	**2.95**	2.90
2020	Jan	3.25	3.32	**2.82**	**2.44**	2.78	**2.64**	**2.82**	2.80
	Feb	2.80	2.95	2.80	**2.38**	2.84	**2.60**	**2.70**	2.87
	Mar	2.67	2.76	**2.44**	**2.44**	**2.63**	**2.50**	**2.62**	**2.57**
	Apr	2.96	**2.35**	**2.52**	**2.23**	**2.32**	2.51	**2.33**	**1.94**
	May	**2.37**	**2.40**	**2.42**	2.30	2.51	2.59	2.66	2.60
	Jun	**2.59**	**2.50**	**2.37**	2.78	2.81	2.44	2.41	2.56
	Jul	**2.76**	**2.80**	2.94	3.56	3.42	4.07	2.64	2.94
	Aug	4.27	3.75	3.47	5.55	4.57	5.20	4.17	3.91
	Sep	4.09	3.66	3.98	5.10	4.38	**3.89**	3.99	4.22
	Oct	3.35	3.29	3.31	**3.02**	3.32	**2.88**	3.47	**3.23**
	Nov	3.31	**3.12**	**3.11**	**2.54**	**2.88**	**3.00**	3.40	**3.05**
	Dec	**2.87**	**2.77**	**2.68**	**2.54**	3.38	**2.84**	3.38	3.17
Annual average	2005–2019	**2.97**	2.99	2.94	**2.90**	**2.94**	**3.03**	**3.04**	**2.94**
	2020	3.11	**2.97**	**2.90**	3.07	3.15	3.10	3.05	2.99

Numbers in red indicate lower concentrations of NO_2 in comparison to 2020, with the average values obtained for the period from 2005 to 2019

3.3 Annual modeling of NO_2 concentration as a function of meteorological parameters

Table 6 presents the following parameters of the PCA adjustment: the KMO index, p value of the sphericity test, explained variance, and the eigenvalues of the first two main components, which are PC1 and PC2, respectively. The values of KMO are greater than 0.5, except for Ponta Porã and Dourados, and p values for Bartlett's sphericity test are less than 0.05, that suggest there is substantial correlation in the data. Hence, data are appropriate for applying PCA. Figure 5 shows individual variables from the output of the PCA analysis. The first main component, for all cities, is able to explain percentages ranging between 51 and 57, while the second component explains percentages ranging between 35 and 47% of the data variance. Therefore, the first two main components can explain a percentage greater than 89% of the data variance. In PC1, for all cities, eigenvectors were positive for NO_2 and negative for Prec and RH. T_{max} and T_{min} were positive for four cities: Dourados, Corumbá, Ponta Porã and Chapadão do Sul, and negative for four others: Campo Grande, Três Lagoas, Coxim and Porto Murtinho.

Overall, the eigenvectors are elevated for all variables, indicating that PC1 is an overview of the relationship between meteorological variables and NO_2 concentration, in which the higher the RH and Prec, the lower the NO_2 concentrations. The role of temperature is ambiguous, indicating that in cities where these variables had positive/negative eigenvectors, the highest temperatures are associated with the highest/lowest concentrations of NO_2. Higher scores indicate places with higher concentrations of NO_2, lower precipitations and relative humidity. These results also reaffirm the seasonal factor of NO_2 concentrations, which are mainly related to humid climatic conditions (Hua et al. 2021). The scores are higher from July through August, the driest months of the year. The higher temperatures and RH in the atmosphere, which occur during summers in MS, are typically beneficial for the removal of NO_2 through

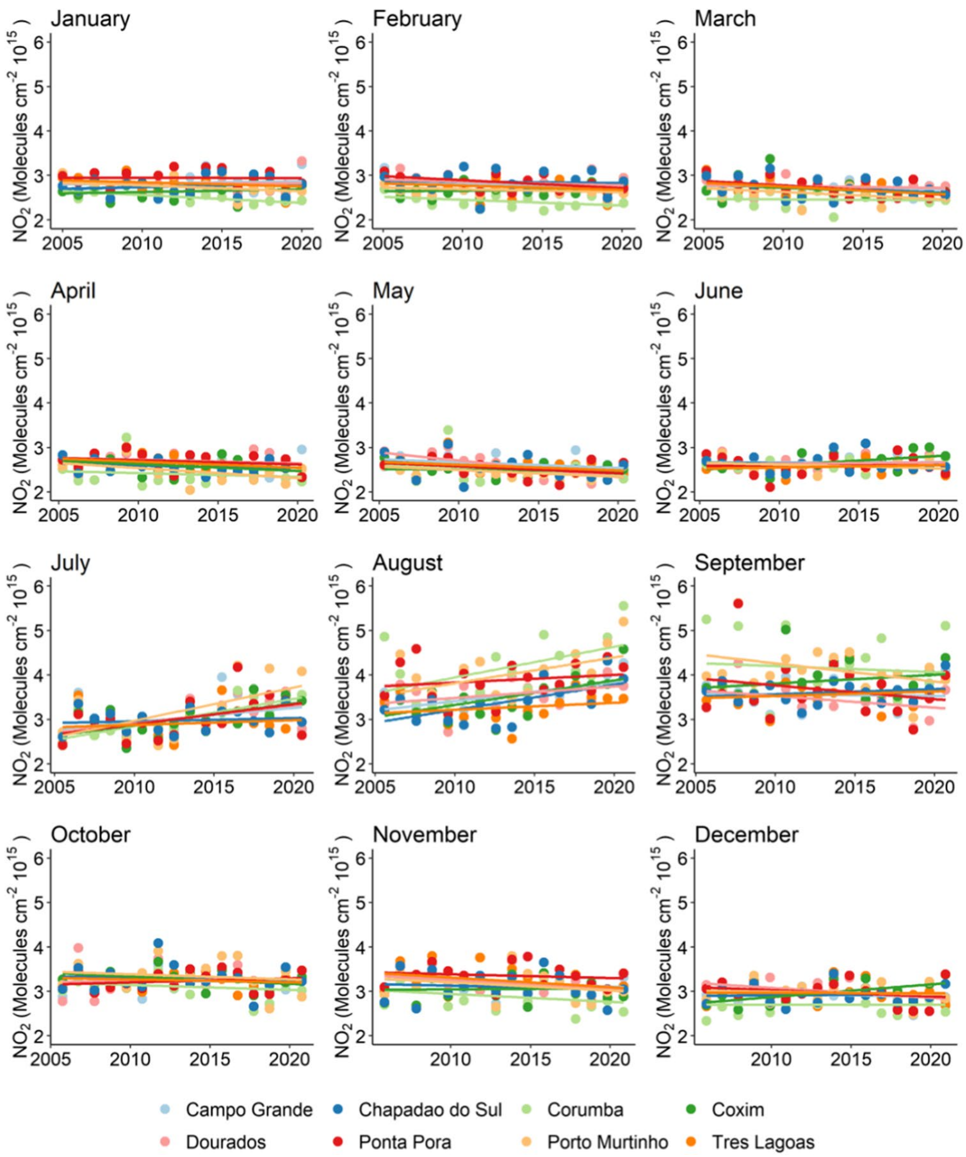

Fig. 4 Dispersion of NO_2 concentration for eight cities of South Mato Grosso in function of the years and the consequent regression lines

Table 5 Mann–Kendall results for relevant months and cities of South Mato Grosso, Tau value, Sen's slope, and year of break of time series of NO_2 concentration

City	Month	Z MK	*p* value	Tau	Sen's slope	Break point
South Chapadão	May	−4.4421	0.0000	−0.2667	−0.0205	2014
Corumbá	Jan	−7.1104	0.0170	−0.4500	−0.0161	2012
Corumbá	Jul	6.3798	0.0034	0.5500	0.0697	2014
Coxim	Jul	5.9227	0.0170	0.4500	0.0508	2012
Coxim	Aug	3.0529	0.0217	0.4333	0.0399	2014
Coxim	Dec	6.3102	0.0170	0.4500	0.0326	2010
Dourados	May	−9.4450	0.0005	−0.6500	−0.0373	2012
Ponta Porã	Feb	−6.2314	0.0428	−0.3833	−0.0197	2012
Porto Murtinho	Apr	−5.2228	0.0000	−0.3167	−0.0226	2010
Porto Murtinho	May	−3.9239	0.0001	−0.3500	−0.0148	2011

Table 6 Parameters of the analysis of main components and the eigenvectors of the first two main components

Cities	KMO	*p* value Bartlett's Sphericity tests	Explained variance		Eigenvectors from PC1					Eigenvectors from PC2				
			PC1	PC2	NO_2	Prec	RH	T_{min}	T_{max}	NO_2	Prec	RH	T_{min}	T_{max}
Campo Grande	0.530	<0.05	0.527	0.452	0.127	−0.603	−0.440	−0.570	−0.319	0.641	0.617	−0.460	0.245	0.561
Dourados	0.485	<0.05	0.511	0.463	0.575	−0.357	−0.549	0.650	0.490	0.226	0.534	0.282	−0.427	0.402
Três Lagoas	0.520	<0.05	0.570	0.352	0.288	−0.553	−0.405	−0.534	−0.403	0.625	−0.601	−0.479	0.287	0.545
Corumbá	0.590	<0.05	0.534	0.430	0.597	−0.180	−0.549	0.108	0.545	0.744	0.635	0.263	0.661	0.298
Coxim	0.560	<0.05	0.568	0.399	0.125	−0.567	−0.324	−0.565	−0.489	0.686	0.817	−0.582	0.198	0.387
Porto Murtinho	0.530	<0.05	0.551	0.407	0.676	−0.575	−0.210	−0.588	−0.525	0.583	−0.105	−0.639	0.119	0.329
Ponta Porã	0.450	<0.05	0.557	0.338	0.526	−0.732	−0.495	0.391	0.570	0.301	−0.426	−0.214	−0.565	0.425
Chapadão do Sul	0.520	<0.05	0.533	0.445	0.340	0.472	−0.664	0.586	0.562	0.545	−0.411	0.742	−0.173	0.252

PC1 and PC2 = principal component 1 and 2, respectively, KMO = Kaiser–Meyer–Olkin parameter, NO_2 = concentration of NO_2 (10^{15} molecules/cm^2), T_{max} = maximum temperature (°C) and T_{min} = minimum temperature (°C), RH = relative humidity (%) and Prec = precipitation (mm)

Photolysis (Feng et al. 2001; Dong et al. 2009). Nevertheless, at some cities (Dourados, Corumbá, Ponta Porã and Chapadão do Sul, the lower temperatures would be allied with lower concentrations of NO_2.

PC2 also originated higher eigenvectors for almost all variables in all cities varying its pattern among cities, i.e., presenting positive and negative eigenvector values. In general, this component indicates the driest months with the highest scores and the most humid months with the lowest scores. Its eigenvectors for NO_2 is always positive. Thus, PC2 indicates differences in the dynamics of NO_2 throughout the atmosphere of every region of MS. Generally, moisture and precipitation are NO_2 dispersing agents (Cai et al. 2018), as well as high temperatures cause NO_2 photolysis, reducing its concentration (Feng et al. 2001; Dong et al. 2009).

The correlation of meteorological elements with the concentration of atmospheric NO_2 can be modeled using the multivariate data technique, represented by the eigenvectors of Table 6, avoiding multi-collinearity in regression models that would include several factors correlated not merely with their response of variable NO_2, but also to each other through weather variables. Therefore, it is possible to estimate meteorological patterns and to establish scores for each month through meteorological variables, by recognizing higher concentrations of atmospheric NO_2.

4 Conclusion

Both the satellite and the terrestrial NO_2 data sets of measurements for MS-Brazil from 2005 to 2020 present basic levels during the rainy season, which occurs from October and March, and maximum levels during the dry season from April to August. The study shows high relative humidity in the MS from October to March, which contributes to the removal of pollutants such as NO_2. Temperature is also an important factor during a few hours due to the photochemical effect that produce OH radicals, which reacts with NO_2 causing it to sink in terms of HNO_3. Climatic seasonality is, therefore, an influencing factor in the atmospheric specifications of NO_2.

Additionally, biomass-burning activities, especially during the driest period of the year, contribute to the increase of atmospheric pressure followed by an increase of NO_2 concentration. Burning of areas for cleaning and subsequent implantation of agricultural crops is notable in South Mato Grosso. Even during the COVID-19 pandemic, the levels of pollutant were similar to those of previous years, with the exception of months in which there were more important restrictions of commercial and industrial activities. The largest tropospheric and total NO_2 concentrations occurred in industrialized and highly agglomerated regions. The highest

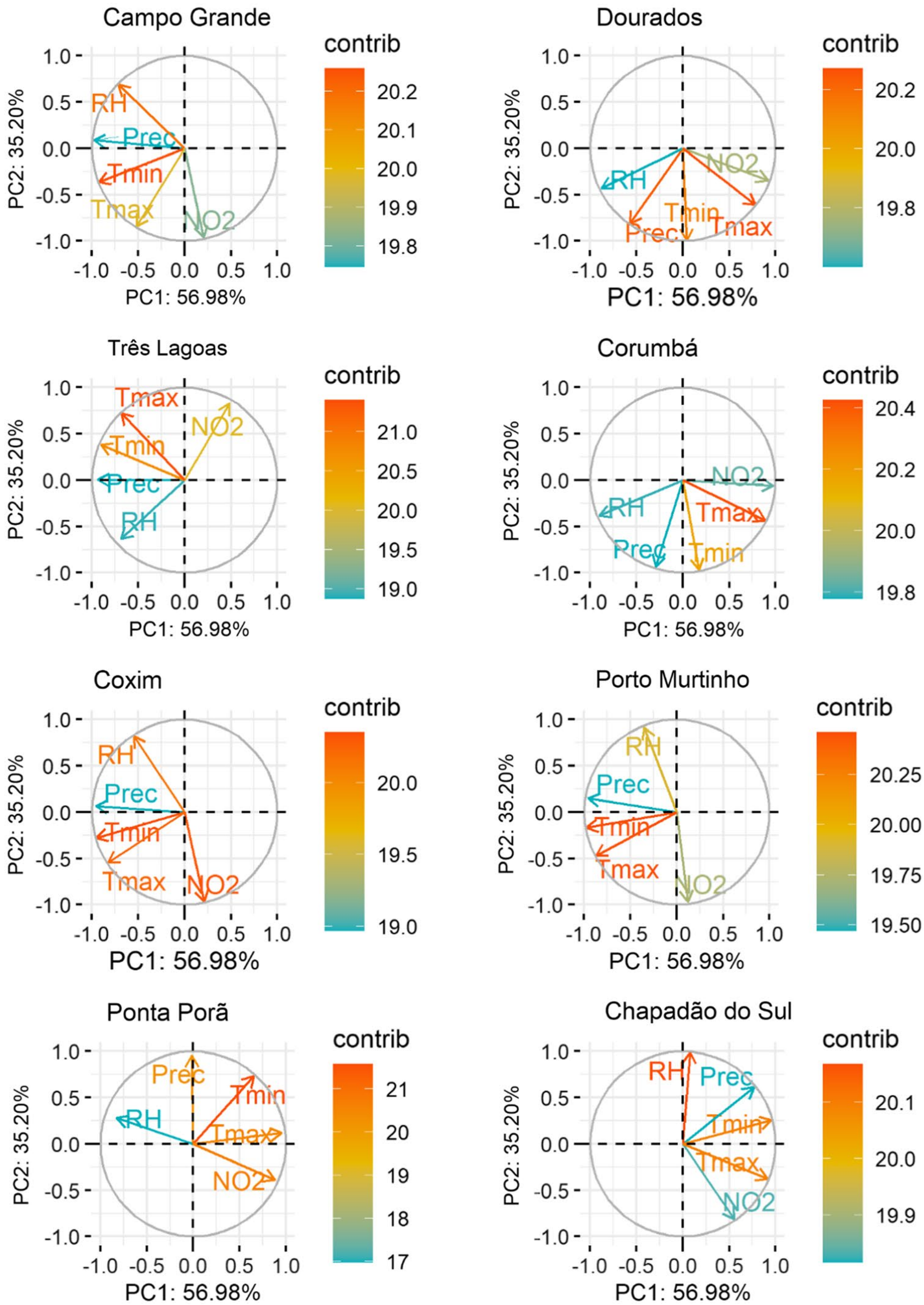

Fig. 5 Individual variables from the output of Principal Component Analysis (ACP) of the cities of South Mato Grosso

NO_2 rules were also observed in biomass burning regions, the trend is not explained as a whole. They reflect differences in trends of variations due to anthropogenic connections of NO_x in the regions.

It has been investigated stationarity in the regional NO_2 column time series and some trends have been found. It is especially noteworthy that trends of increasing NO_2 concentration occur in drier months of the year at some cities. The results demonstrate that the NO_2 of the tropospheric column increased by around 3% and the breaking point of the series varied from 2010 to 2014.

This study successfully produced the analysis of the vertical column of tropospheric NO_2 with values that are smooth and consistent in terms of space and time. A multivariate approach using eigenvectors to predict the NO_2 rules has been applied. The main components within 89% variance of the explained data and the eigenvectors are coherent to climatic seasonality and the mandatory application of NO_2.

Satellite data can be used to assess spatial and temporal variations of NO_2. The integration of satellite inclusion with terrestrial data provides an overview of NO_2 in the atmosphere, which is an essential tool for quality managers and politicians to understand the spatial distribution of air quantities to define air quality policy and mitigation plan for South Mato Grosso.

Supplementary Information The online version contains supplementary material available at https://doi.org/10.1007/s00703-021-00855-5.

Acknowledgements The authors would like to thank the universities for their support. F. Aristone thanks the CNPq—Brazil for financial support.

Author contributions All authors participated in the preparation of the review and writing of the project, data collection, data analysis and writing of the article, review and writing of the article and review of the article.

Funding This study was funded by cnpq (309681/2019-7).

Data availability This research was supported by the Universities and by the UFMS Air Quality Laboratory. We would like to acknowledge the use of data from the tropospheric NO_2 column at http://aura.gsfc.nasa.gov/lindex.html.

Declarations

Conflict of interest The authors declare no conflicts of interest.

References

Abreu MC, Souza A, Lyra GB, Pobocikova I, Cecílio RA (2020) Analysis of monthly and annual rainfall variability using linear models in the state of South Mato Grosso, Midwest of Brazil. Int J Climatol 41:E2445–E2461. https://doi.org/10.1002/joc.6857

Alvares CA, Stape JL, Sentelhas PC, Gonçalves JLM, Sparovek G (2013) Köppen's climate classification map for Brazil. Meteorol Z 22:711–728. https://doi.org/10.1127/0941-2948/2013/0507

Burn DH, Mansour R, Zang K, Whitfield PH (2011) Trends and Variability in Extreme Rainfall Events in British Columbia, Canadian Water Resources Journal / Revue canadienne des ressources hydriques 36(1):67-82. https://doi.org/10.4296/cwrj3601067

Cai K, Zhang Q, Li S, Li Y, Ge W (2018) Spatial–temporal variations in NO_2 and $PM_{2.5}$ over the Chengdu-Chongqing Economic Zone in China during 2005–2015 based on satellite remote sensing. Sensors 18:3950. https://doi.org/10.3390/s18113950

Castellanos P, Boersma KF (2012) Reductions in nitrogen oxides over Europe driven by environ- mental policy and economic recession. Sci Rep 2:1–7. https://doi.org/10.1038/srep00265

Caúla RH, Oliveira-Júnior JF, Lyra GB, Delgado RC, Heilbron Filho PFL (2015) Overview of fire foci causes and locations in Brazil based on meteorological satellite data from 1998 to 2011. Environ Earth Sci 74:1497–1508. https://doi.org/10.1007/s12665-015-4142-z

Dobber MR, Dirksen RJ, Levelt PF, van den Oord GH, Voors RH, Kleipool Q, & Rozemeijer NC (2006). Ozone monitoring instrument calibration. IEEE Transactions on Geoscience and remote Sensing, 44(5):1209-1238. https://doi.org/10.1109/TGRS.2006.869987

Dong J, Wang S, Shang K (2009) Influence of precipitation on air quality in several cities of China. J Arid Land Resour Environ 23:43–48

Drosoglou T, Koukouli ME, Kouremeti N, Bais AF, Zyrichidou I, Balis D, Van der ARJ, Xu J, Li A (2018) MAX-DOAS NO_2 observations over Guangzhou, China; ground-based and satellite comparisons. Atmos Meas Tech 11:2239–2255. https://doi.org/10.5194/amt-11-2239-2018

Duncan BN, Yoshida Y, Foy B, Lamsal LN, Streets DG (2013) The observed response of Ozone Monitoring Instrument (OMI) NO_2 columns to NO_x emission controls on power plants in the United States: 2005–2011. Atmos Environ 81:102–111. https://doi.org/10.1016/j.atmosenv.2013.08.068

Fan H, Zhao C, Yang Y (2020) A comprehensive analysis of the spatio-temporal variation of urban air pollution in China during 2014–2018. Atmos Environ 20:117066. https://doi.org/10.1016/j.atmosenv.2019.117066

Fan H, Wang Y, Zhao C, Yang Y, Yang X, Sun Y, Jiang S (2021) The role of primary emission and transboundary transport in the air quality changes during and after the COVID-19 lockdown in China. Geophys Res Lett 48:e2020GL091065. https://doi.org/10.1029/2020GL091065

Fantozzi F, Monaci F, Blanusa T, Bargagli R (2015) Spatio-temporal variations of ozone and nitrogen dioxide concentrations under urban trees and in a nearby open area. Urban Clim 12:119–127. https://doi.org/10.1016/j.uclim.2015.02.001

Feng ZW, Huang YZ, Feng YW, Ogura N, Zhang FZ (2001) Chemical composition of precipitation in Beijing area, Northern China. Water Air Soil Pollut 125:345–356. https://doi.org/10.1023/A:1005287102786

Garrett TJ, Chuanfeng ZC, Novelli PC (2010) Assessing the relative contributions of transport efficiency and scavenging to seasonal variability in Arctic aerosol. Tellus 62B:190–196. https://doi.org/10.1111/j.1600-0889.2010.00453.x

Grajales FJ, Baquero-Bernal A (2014) Inference of surface concentrations of nitrogen dioxide (NO_2) in Colombia from tropospheric columns of the ozone measurement instrument (OMI). Atmósfera 27:193–214. https://doi.org/10.1016/S0187-6236(14)71110-5

Griffin D, Zhao X, McLinden CA, Boersma F, Bourassa A, Dammers E, Degenstein D, Eskes H, Fehr L, Fioletov V, Wolde M (2018) High resolution mapping of nitrogen dioxide with TROPOMI: first results and validation over the Canadian oil sands. Geophys Res Lett 46:1049–1060. https://doi.org/10.1029/2018GL081095

Hagenbjörk A, Malmqvist E, Mattisson K, Sommar NJ, Modig L (2017) The spatial variation of O_3, NO, NO_2 and NO_x and the relation between them in two Swedish cities. Environ Monit Assess 189:161. https://doi.org/10.1007/s10661-017-5872-z

Hua J, Zhang Y, Foy B, Shang J, Schauer JJ, Mei X, Sulaymon ID, Han T (2021) Quantitative estimation of meteorological impacts and the COVID-19 lockdown reductions on NO_2 and $PM_{2.5}$ over the Beijing area using Generalized Additive Models (GAM). J Environ Manage 291:112676. https://doi.org/10.1016/j.jenvman.2021.112676

Irie H, Muto T, Itahashi S, Kurokawa JI, Uno I (2016) Turnaround of tropospheric nitrogen di-oxide pollution trends in China, Japan, and South Korea. Sola 12:170–174. https://doi.org/10.2151/sola.2016-035

Jiang S, Zhao C, Fan H (2021) Toward understanding the variation of air quality based on a comprehensive analysis in hebei province under the influence of COVID-19 lockdown. Atmosphere 12:267. https://doi.org/10.3390/atmos12020267

Kendall MG (1975) Rank correlation methods. Griffin, London, p 272

Kengni L, Mboussop AN, Kopa AN, Tankou CM, Tematio P, Ngoupayou JRN (2019) Rainfall variability on the southern slope of the Bambouto mountain (West-Cameroon) and impact on the crop cultivation calendar. Journal of African Earth Sciences 154:164–171. https://doi.org/10.1016/j.jafrearsci.2019.03.020

Khokhar MF, Yasmin N, Fatima N, Beirle S, Wagner T (2015) Detection of trends and seasonal variation in tropospheric nitrogen dioxide over Pakistan. Aerosol Air Qual Res 15:2508–2524. https://doi.org/10.4209/aaqr.2015.03.0157

Lamsal LN, Martin RV, Donkelaar AV, Celarier EA, Buscela EJ, Boersma KF, Dirksen R, Luo C, Wang Y (2010) Indirect validation of tropospheric nitrogen dioxide retrieved from the OMI satellite instrument: insight into the seasonal variation of nitrogen oxides at northern Midlatitudes. J Geo Res 115:458–473. https://doi.org/10.1029/2009JD013351

Lelieveld J, Beirle S, Hörmann C, Stenchikov G, Wagner T (2015) Abrupt recent trend changes in atmospheric nitrogen dioxide over the Middle East. Sci Adv 1:e1500498. https://doi.org/10.1126/sciadv.1500498

Levelt PF, Oord GHJVG, Dobber MR (2006) The ozone monitoring instrument. IEEE T Geosci Remote Sens 44:1093–1101

Mann HB (1945) Nonparametric tests against trend. Econometrica J. Econometr. Soc. 13:245–259. https://doi.org/10.2307/1907187

Mele M, Magazzino C, Scheneider N, Strezov V (2021) NO_2 levels as a contributing factor to COVID-19 deaths: the first empirical estimate of threshold values. Environ Res 194:110663. https://doi.org/10.1016/j.envres.2020.110663

Nakada LYK, Urban RC (2020) COVID-19 pandemic: impacts on the air quality during the partial lockdown in São Paulo state, Brazil. Sci Total Environ 730:139087. https://doi.org/10.1016/j.scitotenv.2020.139087

Oliveira Júnior JF, Teodoro PE, Silva Junior CA, Baio FHR, Gava R, Capristo-Silva GF, Gois G, Correia Filho WLF, Lima M, Santiago DB, Freitas WK, Santos PJ, Costa MS (2020) Fire foci related to rainfall and biomes of the state of South Mato Grosso, Brazil. Agric Meteorol 282–283:107861. https://doi.org/10.1016/j.agrformet.2019.107861

Ossohou M, Galy-Lacaux C, Yoboué V, Hickman JE, Gardrat E, Adon M, Darras A, Laouali D, Akpo A, Diop B, Opepa C (2019) Trends and seasonal variability of atmospheric NO_2 and HNO_3 concentrations across three major African biomes inferred from long-term series of ground-based and satellite measurements. Atmos Environ 207:148–166. https://doi.org/10.1016/j.atmosenv.2019.03.027

Pettitt AN (1979) A non-parametric approach to the change-point problem. J R Stat Soc Series C (appl Stat) 28:126–135. https://doi.org/10.2307/2346729

Richter A, Burrows JP, Nüß H, Granier C, Niemeier U (2005) Increase in tropospheric nitrogen dioxide over China observed from space. Nature 437:129–132. https://doi.org/10.1038/nature04092

Sa'adi Z, Shahid S, Ismail T, Chung ES, Wang XJ (2019) Trends analysis of rainfall and rainfall extremes in Sarawak, Malaysia using modified Mann–Kendall test. Meteorol Atmos Phys 131:263–277. https://doi.org/10.1007/s00703-017-0564-3

Schneider P, Van der ARJ (2012) A global single-sensor analysis of 2002–2011 tropospheric nitrogen dioxide trends observed from space. J Geophys Res: Atmos 117(D16):1–17. https://doi.org/10.1029/2012JD017571

Sen PK (1968) Estimates of the regression coefficient based on Kendall's tau. J Am Stat Assoc 63:1379–1389

Shi JP, Harrison RM (1997) Regression modelling of hourly NO_x and NO_2 concentrations in urban air in London. Atmos Environ 31:4081–4094. https://doi.org/10.1016/S1352-2310(97)00282-3

Silva Junior CA, Teodoro PE, Delgado RC, Teodoro LPR, Lima M, Pantaleão AA, Baio FHR, Azevedo GB, Azevedo GTOS, Capristo-Silva GF, Arvor D, Facco CU (2020) Persistent fire foci in all biomes undermine the Paris Agreement in Brazil. Sci Rep 10:16246. https://doi.org/10.1038/s41598-020-72571-w

Souza A, Fernandes WA, Albrez EA, Galvíncio JD (2012) Análise de Agrupamento da Precipitação e da Temperatura no South Mato Grosso. Acta Geo 6:109–124. https://doi.org/10.5654/acta.v6i12.782

Souza A, Aristone F, Garcia AP, Santos DA, Nóbrega S (2018a) Estudo da associação entre óxidos de nitrogênio e concentração de ozônio com parâmetros meteorológicos. Geosul 33:164–183. https://doi.org/10.5007/2177-5230.2018v33n68p164

Souza A, Ikefuti PV, Garcia AP, Santos DAS, Oliveira S (2018b) Análise da Relação Entre O_3, NO e NO_2 Usando Técnicas de Regressão Linear Múltipla. Geograph 20:124. https://doi.org/10.22409/GEOgraphia2018.v20i43.a27215

Teodoro PE, Oliveira-Júnior JF, Cunha ER, Correa CCG, Torres FE, Bacani VM, Gois G, Ribeiro LP (2016) Cluster analysis applied to the spatial and temporal variability of monthly rainfall in South Mato Grosso State, Brazil. Meteorol Atmos Phys 128:197–209. https://doi.org/10.1007/s00703-015-0408-y

Tomei J, Lyrio de Oliveira L, Oliveira Ribeiro C, Lee Ho L, Montoya LG (2020) Assessing the relationship between sugarcane expansion and human development at the municipal level: a case study of South Mato Grosso, Brazil. Bio Bioener 141:105700. https://doi.org/10.1016/j.biombioe.2020.105700

Torres O, Ahn C, Chen Z (2013) Improvements to the OMI near-UV aerosol algorithm using A-train CALIOP and AIRS observations. Atmos Meas Tech 6:3257–3270. https://doi.org/10.5194/amt-6-3257-2013

Ul-Haq Z, Rana AD, Tariq S, Mahmood K, Ali M, Bashir I (2018) Modeling of tropospheric NO_2 column over different climatic zones and land use/land cover types in South Asia. J Atmos Sol Ter Phys 168:80–99. https://doi.org/10.1016/j.jastp.2018.01.022

Uliana EM, Silva DD, Uliana EM, Rodrigues BS, Corrêdo LP (2015) Análise de tendência em séries históricas de vazão e precipitação: uso de teste estatístico não paramétrico. Rev Ambient Água 10:82–88. https://doi.org/10.4136/ambi-agua.1427

Wang Z, Uno I, Yumimoto K, Itahashi S, Chen X, Yang W, Wang Z (2021) Impacts of COVID-19 lockdown, Spring Festival and meteorology on the NO_2 variations in early 2020 over China based on in-situ observations, satellite retrievals and model simulations. Atmos Environ 244:117972. https://doi.org/10.1016/j.atmosenv.2020.117972

Xiao K, Wang Y, Wu G, Fu B, Zhu Y (2018) Spatiotemporal characteristics of air pollutants (PM_{10}, $PM_{2.5}$, SO_2, NO_2, O_3, and CO) in the inland basin city of Chengdu, Southwest China. Atmosphere 9:74–90. https://doi.org/10.3390/atmos9020074

Xue R, Wang S, Li D, Zou Z, Chan KL, Valks P, Saiz-Lopez A, Zhou B (2020) Spatio-temporal variations in NO_2 and SO_2 over Shanghai and Chongming Eco-Island measured by Ozone Monitoring Instrument (OMI) during 2008–2017. J Clean Prod 258:120563. https://doi.org/10.1016/j.jclepro.2020.120563

Yanfang H, Litao W, Yi Z, Shixin W, Cong D, Feng W (2019) Spatiotemporal variations of tropospheric column nitrogen dioxide over Jing-Jin-Ji during the past decade. Int J Remote Sens 40:15–30. https://doi.org/10.1080/01431161.2018.1463115

Yavaşlı DD (2020) Spatio-temporal Variations of tropospheric nitrogen dioxide in Turkey based on satellite remote sensing. Geo Pan 24:168–175. https://doi.org/10.5937/gp24-25482

Yue S, Wang C (2004) The Mann–Kendall test modified by effective sample size to detect trend in serially correlated hydrological series. Water Resour Manag 18:201–218. https://doi.org/10.1023/B:WARM.0000043140.61082.60

Zeri M, Oliveira-Júnior JF, Lyra GB (2011) Spatiotemporal analysis of particulate matter, sulfur dioxide and carbon monoxide concentrations over the city of Rio de Janeiro, Brazil. Meteorol Atmos Phys 113:139–152. https://doi.org/10.1007/s00703-011-0153-9

Zeri M, Carvalho VSB, Cunha-Zeri G, Oliveira-Júnior JF, Lyra GB, Freitas ED (2016) Assessment of the variability of pollutants concentration over the metropolitan area of São Paulo, Brazil, using the wavelet transform. Atmos Sci Lett 17:87–95. https://doi.org/10.1002/asl.618

Zhang Y, Ma Z, Gao Y, Zhang M (2021) Impacts of the meteorological condition versus emissions reduction on the PM2.5 concentration over Beijing–Tianjin–Hebei during the COVID-19 lockdown. Atmos. Oceanic Sci. Lett. 14:100014. https://doi.org/10.1016/j.aosl.2020.100014

Zhao X, Sun Y, Zhao C, Jiang H (2020) Impact of precipitation with different intensity on $PM_{2.5}$ over typical regions of China. Atmosphere 11:906. https://doi.org/10.3390/atmos11090906

Zheng C, Zhao C, Li Y, Wu X, Zhang K, Gao J, Qiao Q, Ren Y, Zhang X, Chai F (2018) Spatial and temporal distribution of NO_2 and SO_2 in Inner Mongolia urban agglomeration obtained from satellite remote sensing and ground observations. Atmos Environ 188:50–59. https://doi.org/10.1016/j.atmosenv.2018.06.029